

Article

A Comparative Study on Steady-State Water Inflow into a Circular Underwater Tunnel with an Excavation Damage Zone

Yi-Heng Pan ^{1,*}, Jia-Rui Qi ¹, Jin-Feng Zhang ², Ya-Xiong Peng ³, Chao Chen ¹, Hai-Nan Ma ¹ and Chen Ye ¹¹ College of Harbour and Coastal Engineering, Jimei University, Xiamen 361021, China² State Key Laboratory of Hydraulic Engineering Simulation and Safety, Tianjin University, Tianjin 300072, China³ Hunan Provincial Key Laboratory of Geotechnical Engineering for Stability Control and Health Monitoring, School of Civil Engineering, Hunan University of Science and Technology, Xiangtan 411100, China

* Correspondence: panyiheng@jmu.edu.cn

Abstract: Excavation damage zones that occur around tunnels usually lead to a change in rock permeability, which has an impact on the water inflow into tunnels and even induces water inrush disasters. For a better understanding of the effect of the excavation damage zone, analytical solutions that consider the excavation damage zone are developed based on the review and modification of the solutions that consider linings and grouting circles. Then, both analytical solutions and the finite element method are applied to estimate the water inflow, and the results are in good agreement. The effect of the excavation damage zone on water inflow is analyzed based on an impact factor of the excavation damage zone and evaluated in a real engineering case, and the seepage-preventing effects of grouting are discussed. The results reveal that the water inflow increases with increasing permeability and thickness of the excavation damage zone and that there is a limit for the effects of the excavation damage zone. In addition, the effect is stronger for underwater tunnels with small water inflows and stabilizes gradually as the magnitude of water inflow increases. The increase in the impermeability and thickness of the lining and grouting circle can reduce the effect.

Keywords: underwater tunnel; water inflow; analytical solutions; numerical method; excavation damage zone



Citation: Pan, Y.-H.; Qi, J.-R.; Zhang, J.-F.; Peng, Y.-X.; Chen, C.; Ma, H.-N.; Ye, C. A Comparative Study on Steady-State Water Inflow into a Circular Underwater Tunnel with an Excavation Damage Zone. *Water* **2022**, *14*, 3154. <https://doi.org/10.3390/w14193154>

Academic Editor: Giuseppe Pezzinga

Received: 27 August 2022

Accepted: 2 October 2022

Published: 7 October 2022

Publisher's Note: MDPI stays neutral with regard to jurisdictional claims in published maps and institutional affiliations.



Copyright: © 2022 by the authors. Licensee MDPI, Basel, Switzerland. This article is an open access article distributed under the terms and conditions of the Creative Commons Attribution (CC BY) license (<https://creativecommons.org/licenses/by/4.0/>).

1. Introduction

As an important option of underwater transportation engineering, underwater tunnels have the advantages of insensitivity to weather, no obstruction of navigation, good seismic performance and little impact on ecosystems. Hence, a considerable number of underwater tunnels have been constructed in the past century [1–3]. The estimation of water inflow is a key and difficult issue for underwater tunnels due to infinite water supply and defects of water-proofing systems [4–7]. Many efforts have been devoted to proposing effective methods to predict water inflow into tunnels over the past few decades. Four kinds of methods, including analytical solutions [8–14], numerical simulations [15–19], empirical formulas [20,21] and physical experiments [22], have been applied to estimate water inflow into tunnels.

Analytical solutions have some advantages, namely, convenience, reliability, and low cost [23]. Therefore, many researchers have developed various analytical solutions to predict water inflow into tunnels. Based on the image method proposed by Harr [24], a series of analytical solutions were derived for water inflow into tunnels in an infinite or semi-infinite aquifer [10,25–27]. In addition, there are several analytical and semianalytical solutions that consider the influence of lining, grouting and drawdown based on a multidomain model or numerical simulations [6,8,28]. Conformal mapping is another widely used method to obtain analytical solutions by transforming a semi-infinite aquifer into an annular or rectangular domain [23,29–31]. This method can deal with different boundary

conditions (zero water pressure and constant total head) along the tunnel circumference and has drawn much attention from researchers. Some novel analytical solutions that consider the effects of various factors, such as lining and grouting, have been proposed based on conformal mapping [32–36]. Compared with the analytical solution, the numerical method can provide the ability to handle more complex geological and hydrological models and boundary conditions [13,14]. A number of studies on water inflow into tunnels using numerical methods have been conducted, and the effects of various factors on water inflow have been investigated synthetically [5,7,14,37].

It is worth noting that the formation of an excavation damage zone (EDZ) is expected to occur around tunnels due to excavation, and the EDZ is characterized by increased fractures, which lead to a significant increase in rock permeability [12,37–40]. This argument is supported by several field measurements, as follows: Souley et al. [41] reported hydraulic experiments by Canada's Underground Research Laboratory, and the results indicated that the permeability of the EDZ can be increased by approximately 5 orders of magnitude, compared with the original rock. The results of field measurements in the Opalinus clay of the Mont Terri Rock Laboratory showed that the average hydraulic conductivity of the surrounding rock within 10–20 cm behind the lining increased by 2–4 orders of magnitude [42]. Tsang et al. [40] reported an increase in the permeability of the EDZ of up to 6 orders of magnitude for a tunnel excavated in indurated clays.

However, few of the aforementioned studies have considered the negative impact of the EDZ on water inflow into tunnels in a semi-infinite aquifer. Hence, a comparative study on steady-state water inflow into a circular underwater tunnel with an EDZ is conducted based on both analytical solutions and numerical methods. First, the analytical solutions for water inflow into a circular underwater tunnel with an EDZ in a semi-infinite aquifer have been proposed, based on the review and modification of the analytical solutions for a circular tunnel with a lining and grouting circle. Subsequently, the finite element method (FEM) is applied to estimate the water inflow into a circular underwater tunnel with an EDZ, and the calculation results of both the analytical solutions and numerical method are compared. Finally, the effect of the EDZ on water inflow into the tunnel is analyzed based on an impact factor of the EDZ proposed in this study and evaluated in the real engineering case reported in the literature, and the seepage-preventing effects of grouting are discussed.

2. Analytical Solutions

A simplified model of a circular underwater tunnel with an EDZ in a semi-infinite aquifer with a horizontal water level is shown in Figure 1. Hassani et al. [18] summarized some simplified assumptions presented in previous studies on analytical solutions for steady-state water inflow into tunnels. These simplified assumptions are modified and applied in this study as follows:

The properties of the surrounding rock, lining and EDZ are homogeneous and isotropic. The water flow is steady-state, incompressible and governed by Darcy's law. The tunnel cross-section is circular, and the water level is horizontal.

Since the media are isotropic and homogeneous, the seepage field can be described by the following Laplace equation according to Darcy's law and mass conservation:

$$\frac{\partial^2 \phi}{\partial x^2} + \frac{\partial^2 \phi}{\partial y^2} = 0 \quad (1)$$

where ϕ is the total head that can be expressed as follows:

$$\phi = \frac{p}{\gamma_w} + y + h \quad (2)$$

where p is the water pressure, γ_w is the unit weight of water, and $y + h$ is the elevation head.

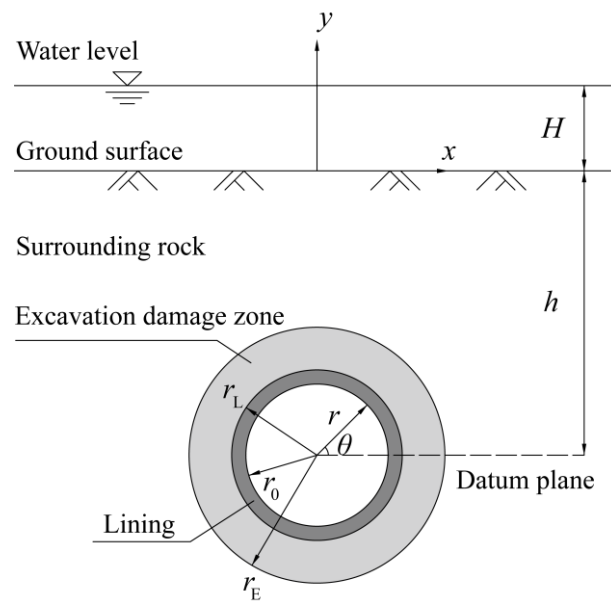


Figure 1. Simplified model of a circular underwater tunnel with an EDZ in a semi-infinite aquifer with a horizontal water level: H , depth from the water level to the ground surface; h , depth from the ground surface to the tunnel center; r_0 , internal radius of the tunnel; r_L , radius of the tunnel with lining; r_E , radius of the tunnel with lining and the EDZ.

The boundary condition at the ground surface is expressed as

$$\phi_{(y=0)} = H + h \tag{3}$$

In the case of a circular underwater tunnel, two different boundary conditions along the inner circumference of the lining were used in previous studies [29–31], as follows:

$$\phi_{(r=r_0)} = h_a \tag{4}$$

$$\phi_{(r=r_0)} = \frac{u_a}{\gamma_w} + y + h \tag{5}$$

where h_a is the constant total head on the inner circumference of the lining and u_a is the constant water pressure on the inner circumference of the lining.

Considering the similarity of the EDZ and grouting circle, those analytical solutions for a circular tunnel with a lining and grouting circle in a semi-infinite aquifer with a horizontal water level can be modified and used to investigate the effect of the EDZ on water inflow into the tunnel by replacing the grouting circle with the EDZ. A brief description of the related analytical solutions can be outlined as follows:

Yang et al. [8] proposed analytical solutions for steady-state water inflow into a circular tunnel with linings and grouting circles in a semi-infinite aquifer, as follows:

$$Q = 2\pi \frac{H + h}{\frac{1}{k_G} \ln \frac{r_G}{r_L} + \frac{1}{k_L} \ln \frac{r_L}{r_0} + \frac{1}{k_R} \ln \frac{h}{r_G}} \tag{6}$$

where Q is the steady-state water inflow into a circular tunnel, and k_R , k_L , k_G are the permeability coefficients of the surrounding rock, lining, and grouting circle, respectively, and r_G is the radius of the tunnel with the lining and grouting circle.

Equation (6) is developed by considering the surrounding rock as an annular zone with an external radius of h , and the total head on the inner circumference of the lining is zero.

Du et al. [33] and Pan et al. [35] presented analytical solutions for the estimation of steady-state water inflow into a deep tunnel with a lining and grouting circle in a semi-

infinite aquifer by using different conformal mapping methods. The proposed equation, assuming the total head on the inner circumference of lining h_a is constant, is as follows:

$$Q = 2\pi \frac{H + h - h_a}{\frac{1}{k_G} \ln \frac{r_G}{r_L} + \frac{1}{k_L} \ln \frac{r_L}{r_0} + \frac{1}{k_R} \ln \frac{h + \sqrt{h^2 - r_G^2}}{r_G}} \tag{7}$$

Ying et al. [27] adapted the image method to derive a solution with the total head along the inner circumference of the lining of zero, as follows:

$$Q = 2\pi \frac{H + h}{\frac{1}{k_G} \ln \frac{r_G}{r_L} + \frac{1}{k_L} \ln \frac{r_L}{r_0} + \frac{1}{k_R} \ln \frac{2h}{r_G}} \tag{8}$$

Zhu et al. [36] used conformal mapping to study this problem with the assumption of zero water pressure on the inner circumference of the lining, and the solution is as follows:

$$Q = 2\pi \frac{H + h + (A - h)C}{\frac{1}{k_G} \ln \frac{r_G}{r_L} + \frac{1}{k_L} \ln \frac{r_L}{r_0} + \frac{1}{k_R} \ln \frac{h + \sqrt{h^2 - r_G^2}}{r_G}} \tag{9}$$

where $A = \sqrt{h^2 - r_G^2}$ and C is a constant determined by equal seepage velocity at each intersection. The solution process and expression for C are complicated and not described in detail here. The above analytical solutions and their descriptions are listed in Table 1.

Table 1. Analytical solutions for a circular tunnel with lining and grouting circle in a semi-infinite aquifer with a horizontal water table.

Reference	Equation	Description
Yang et al. [8]	$Q = 2\pi \frac{H+h}{\frac{1}{k_G} \ln \frac{r_G}{r_L} + \frac{1}{k_L} \ln \frac{r_L}{r_0} + \frac{1}{k_R} \ln \frac{h}{r_G}}$	Homogeneous and isotropic media For both shallow and deep drained tunnels $\phi_{(r=r_0)} = 0$
Du et al. [33]; Pan et al. [35]	$Q = 2\pi \frac{H+h-h_a}{\frac{1}{k_G} \ln \frac{r_G}{r_L} + \frac{1}{k_L} \ln \frac{r_L}{r_0} + \frac{1}{k_R} \ln \frac{h+\sqrt{h^2-r_G^2}}{r_G}}$	Homogeneous and isotropic media Deep tunnels $\phi_{(r=r_0)} = h_a$
Ying et al. [27]	$Q = 2\pi \frac{H+h}{\frac{1}{k_G} \ln \frac{r_G}{r_L} + \frac{1}{k_L} \ln \frac{r_L}{r_0} + \frac{1}{k_R} \ln \frac{2h}{r_G}}$	Homogeneous and isotropic media Deep drained tunnels $\phi_{(r=r_0)} = 0$
Zhu et al. [36]	$Q = 2\pi \frac{H+h+(A-h)C}{\frac{1}{k_G} \ln \frac{r_G}{r_L} + \frac{1}{k_L} \ln \frac{r_L}{r_0} + \frac{1}{k_R} \ln \frac{h+\sqrt{h^2-r_G^2}}{r_G}}$	Homogeneous and isotropic media For both shallow and deep drained tunnels $\phi_{(r=r_0)} = y + h$

Based on the analytical solutions listed in Table 1, the analytical solutions for a circular tunnel with lining and an EDZ in a semi-infinite aquifer with a horizontal water level can be obtained by replacing the grouting circle with the EDZ, as follows:

$$Q_{A1} = 2\pi \frac{H + h - h_a}{\frac{1}{k_E} \ln \frac{r_E}{r_L} + \frac{1}{k_L} \ln \frac{r_L}{r_0} + \frac{1}{k_R} \ln \frac{h}{r_E}} \tag{10}$$

$$Q_{A2} = 2\pi \frac{H + h - h_a}{\frac{1}{k_E} \ln \frac{r_E}{r_L} + \frac{1}{k_L} \ln \frac{r_L}{r_0} + \frac{1}{k_R} \ln \frac{h + \sqrt{h^2 - r_E^2}}{r_E}} \tag{11}$$

$$Q_{A3} = 2\pi \frac{H + h - h_a}{\frac{1}{k_E} \ln \frac{r_E}{r_L} + \frac{1}{k_L} \ln \frac{r_L}{r_0} + \frac{1}{k_R} \ln \frac{2h}{r_E}} \tag{12}$$

$$Q_{A4} = 2\pi \frac{H + h + (A - h)C}{\frac{1}{k_E} \ln \frac{r_E}{r_L} + \frac{1}{k_L} \ln \frac{r_L}{r_0} + \frac{1}{k_R} \ln \frac{h + \sqrt{h^2 - r_E^2}}{r_E}} \tag{13}$$

where k_E is the permeability coefficient of EDZ.

The constant total head on the inner circumference of lining h_a is applied for Equations (10)–(12). For Equation (13), zero water pressure on the inner circumference of the lining is used, and $A = \sqrt{h^2 - r_E^2}$. It is worth mentioning that a constant internal water pressure that never exceeds the initial water pressure is assumed for a tunnel with lining and a grouting circle [43]. El Tani [29] considered that the constant internal water pressure can be the production of the minimal initial water pressure by a coefficient, as follows:

$$\phi_{(r=r_0)} = y + h + \beta(H + h - r_0) \tag{14}$$

where β is a coefficient that ranges from 0 to 1.

Therefore, the new analytical solution Q_{A4} that corresponds to a constant internal pore pressure can be obtained based on Equations (13) and (14), as follows:

$$Q_{A4} = 2\pi \frac{H + h + (A - h)D - \beta(H + h - r_0)}{\frac{1}{k_E} \ln \frac{r_E}{r_L} + \frac{1}{k_L} \ln \frac{r_L}{r_0} + \frac{1}{k_R} \ln \frac{h + \sqrt{h^2 - r_E^2}}{r_E}} \tag{15}$$

where D is a constant determined by equal seepage velocity at each intersection. Based on the method in reference [36], D and other constants to be determined can be acquired as follows:

$$D = \frac{1}{2} \left[E + (1 - E) \frac{r_0^2}{r_L^2} + \frac{k_L}{k_E} \left(E - (1 - E) \frac{r_0^2}{r_L^2} \right) \right] + \frac{1}{2} \left[E + (1 - E) \frac{r_0^2}{r_L^2} - \frac{k_L}{k_E} \left(E - (1 - E) \frac{r_0^2}{r_L^2} \right) \right] \frac{r_L^2}{r_E^2} \tag{16}$$

$$E = \frac{N_1 + N_2 N_3 - N_4}{N_5 - N_2 N_6} \tag{17}$$

$$N_1 = \frac{H + h - \beta(H + h - r_0)}{\frac{1}{k_E} \ln \frac{r_E}{r_L} + \frac{1}{k_L} \ln \frac{r_L}{r_0} - \frac{1}{k_R} \ln \alpha} \left(\frac{1}{r_E} + \frac{\rho}{\alpha} \right) \tag{18}$$

$$N_2 = \frac{A - h}{\frac{1}{k_E} \ln \frac{r_E}{r_L} + \frac{1}{k_L} \ln \frac{r_L}{r_0} - \frac{1}{k_R} \ln \alpha} \left(\frac{1}{r_E} + \frac{\rho}{\alpha} \right) - 2k_R A \sum_{n=1}^{\infty} \frac{n\alpha^{n-1}(\alpha^{2n} + 1)}{\alpha^{2n} - 1} \rho \tag{19}$$

$$N_3 = \frac{1}{2} \left(\frac{r_0^2 k_E - k_L}{r_L^2} + \frac{r_0^2 k_E + k_L}{r_E^2} \right) \tag{20}$$

$$N_4 = \frac{1}{2} \left(\frac{r_0^2}{r_L^2} (k_E - k_L) - \frac{r_0^2}{r_E^2} (k_E + k_L) \right) \tag{21}$$

$$N_5 = \frac{1}{2} \left(\frac{r_L^2 - r_0^2}{r_L^2} k_E + \frac{r_L^2 + r_0^2}{r_L^2} k_L - \frac{r_L^2 - r_0^2}{r_E^2} k_E + \frac{r_L^2 + r_0^2}{r_E^2} k_L \right) \tag{22}$$

$$N_6 = \frac{1}{2} \left(\frac{r_L^2 - r_0^2}{r_L^2} + \frac{r_L^2 + r_0^2}{r_L^2} \frac{k_L}{k_E} + \frac{r_L^2 - r_0^2}{r_E^2} - \frac{r_L^2 + r_0^2}{r_E^2} \frac{k_L}{k_E} \right) \tag{23}$$

$$\alpha = \frac{r_E}{h + A} \tag{24}$$

$$\rho = -\frac{2A}{(h + r_E + A)^2} \tag{25}$$

Compared with Q_{A1} , Q_{A2} , and Q_{A3} , the boundary conditions along the inner circumference of the lining of Q_{A4} are more realistic. To reveal the difference among these

analytical solutions above, the relative error based on Q_{A4} is calculated by the following equation:

$$\delta_i = \frac{Q_{Ai} - Q_{A4}}{Q_{A4}} \times 100\% \tag{26}$$

where i represents the number of the analytical solution and ranges from 1 to 3.

A series of computational analyses are conducted to obtain δ_i , and the computational parameters are shown in Table 2.

Table 2. Parameters of computational analyses.

Surrounding Rock		EDZ		Lining	
H	0 m, 45 m	r_E	4.5 m	r_L	3 m
h	6~90 m	k_E	1×10^{-5} m/s	r_0	2.4 m
k_R	1×10^{-6} m/s	-	-	k_L	1×10^{-7} m/s, 1×10^{-8} m/s

The following assumptions are applied to make the calculation more concise:

For Equations (10)–(12), the constant total head on the inner circumference of the lining is equal to the total head at the point ($x = \pm r, y = -h$), namely, $h_a = 0$. For Equations (15), the coefficient β is equal to zero, namely, $u_a = 0$.

The difference among analytical solutions with different h/r_E is shown in Figure 2. In Figure 2a,b, δ_1 varies from 2.5% to 3%, δ_2 varies from -0.5% to 1%, and δ_3 varies from -1% to 0.5%, when $k_R/k_L = 100$. In Figure 2c,d, δ_1 varies from 13% to 24%, δ_2 varies from 0% to 3.5%, and δ_3 varies from -4% to 0%, when $k_R/k_L = 10$. The above results indicate that compared with the other solutions, Q_{A1} overestimates the water inflow into the tunnel. δ_1 increases as k_R/k_L decreases and the maximum is close to 24% in this study. The underlying reason is that the surrounding rock is assumed to be an annular zone with an external radius of h to develop Q_{A1} , which is different from the condition of a semi-infinite aquifer.

The calculation results of Q_{A2} , Q_{A3} and Q_{A4} are quite similar, and the maximum of δ is within $\pm 4\%$. δ_2 and δ_3 are relatively large when $h/r_E < 4$, and stabilize at approximately 0% as h/r_E increases because $h + \sqrt{h^2 - r_E^2} \approx 2h$ and the water flow can be approximated as radial when $h \gg r_E$. In addition, the variation in H/r_E has little effect on δ , but the variation in k_R/k_L has a significant effect on δ according to Figure 2. When k_R/k_L decreases from 100 to 10, the mean value of δ_1 increases from 2.8% to 17%, and the maximum values of δ_2 and δ_3 increase by more than three times.

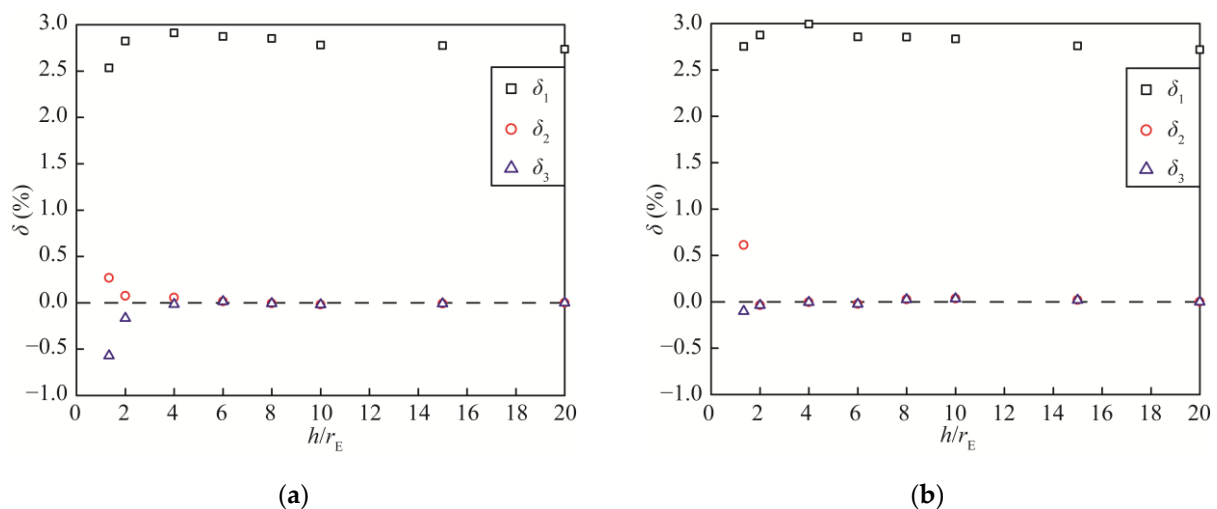


Figure 2. Cont.

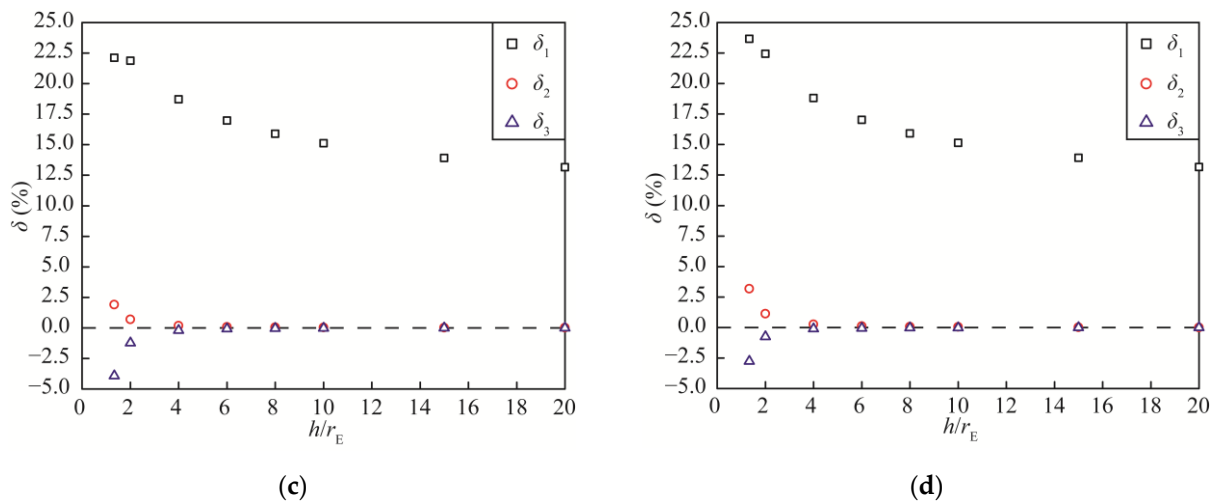


Figure 2. Difference among analytical solutions with different h/r_E in various H/r_E and k_R/k_L values. (a) $H/r_E = 10, k_R/k_L = 100$; (b) $H/r_E = 0, k_R/k_L = 100$; (c) $H/r_E = 10, k_R/k_L = 10$; (d) $H/r_E = 0, k_R/k_L = 10$.

3. Numerical Method

Numerical simulation is one of the most important means to predict the water inflow into a tunnel due to its advantage in dealing with complex models and boundary conditions. A variety of numerical methods have been developed to solve problems for different media [18,19]. Considering the basic assumptions, the finite element method (FEM) is applicable to this study. Hence, the finite element commercial software package ABAQUS (ABAQUS 2021) is used to estimate the steady-state water inflow into a circular tunnel with a lining and an EDZ in a semi-infinite aquifer with a horizontal water level. According to the simplified model shown in Figure 1, a two-dimensional numerical model is created using ABAQUS/CAE 2021, as shown in Figure 3. The geometric parameters and permeabilities of the numerical model are set in the Part module and the Property module of ABAQUS/CAE 2021, according to Table 2. The other descriptions of this numerical model are as follows:

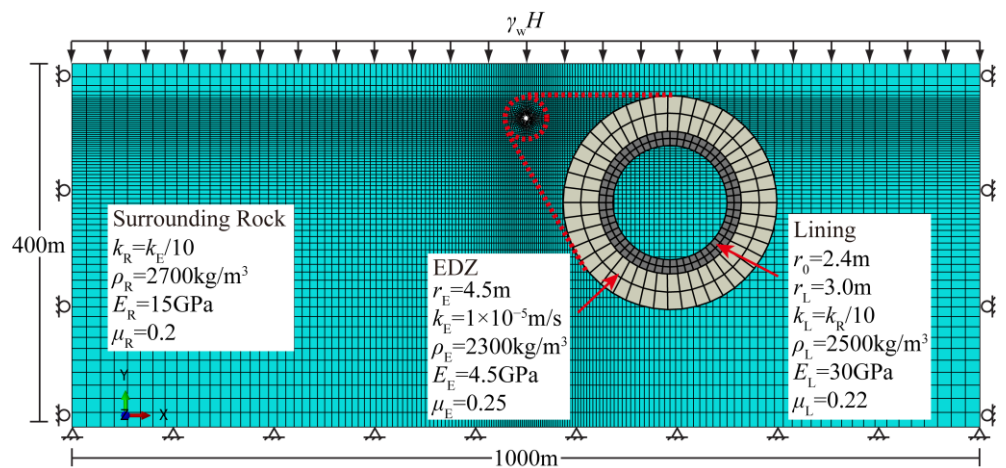


Figure 3. Numerical model for steady-state water inflow into a circular underwater tunnel with lining and an EDZ in a semi-infinite aquifer with a horizontal water level.

An underwater tunnel with a diameter of 6 m is excavated at h m below the ground surface from the tunnel center. The distances from the tunnel center to the bottom and both sides are $(400 - h)$ m and 500 m, respectively, which are more than 50 times the diameter. Therefore, the influence of the boundaries on water inflow can be ignored in this study. Three kinds of materials, including the surrounding rock, EDZ, and lining, are applied in

this model. The Mohr-Coulomb constitutive model is adopted for the surrounding rock and EDZ, and the elastic constitutive model is adopted for the lining.

The boundary conditions of this numerical model are set in the Load module of ABAQUS/CAE 2021 and listed as follows:

The horizontal displacement of both sides is constrained, and the displacement of the bottom is constrained. The bottom boundary is impermeable, and the total heads of both sides are constant. The water pressure on the ground surface is equivalent to a uniformly distributed force ($\gamma_w H$). Three kinds of seepage boundary conditions along the inner circumference of lining are considered in this study, including zero total head ($h_a = 0$), zero water pressure ($\beta = 0$), and non-zero water pressure ($\beta = 0.5$).

The water inflow predicted by numerical simulations is compared with that obtained by the analytical solution, as shown in Table 3. The relative error based on Q_{A4} is calculated by the following equation:

$$\delta_{Ni} = \frac{Q_{Ni} - Q_{A4}}{Q_{A4}} \times 100\% \tag{27}$$

where i represents the number of the numerical simulation and ranges from 1 to 2. Q_{N1} represents the water inflow obtained from the numerical simulation with zero total head along the inner circumference of lining. Q_{N2} represents the water inflow obtained from the numerical simulation with constant water pressure along the inner circumference of the lining.

Table 3. Water inflow by numerical method and analytical solutions.

k_R/k_L	H/r_E	h/r_E	Q_{N1} ($m^3 \cdot d^{-1} \cdot m^{-1}$)	$Q_{N2(\beta=0)}$ ($m^3 \cdot d^{-1} \cdot m^{-1}$)	$Q_{A4(\beta=0)}$ ($m^3 \cdot d^{-1} \cdot m^{-1}$)	$Q_{N2(\beta=0.5)}$ ($m^3 \cdot d^{-1} \cdot m^{-1}$)	$Q_{A4(\beta=0.5)}$ ($m^3 \cdot d^{-1} \cdot m^{-1}$)		
10	10	1.33	8.875	8.861	8.858	4.633	4.630		
		2	8.156	8.149	8.112	4.252	4.233		
		4	7.916	7.913	7.876	4.106	4.087		
		6	8.223	8.222	8.223	4.231	4.248		
		8	8.723	8.721	8.720	4.478	4.488		
		10	9.294	9.293	9.277	4.770	4.762		
		15	10.723	10.722	10.766	5.504	5.497		
		20	12.218	12.217	12.295	6.217	6.257		
		10	0	1.33	1.029	1.031	1.029	0.717	0.716
				2	1.377	1.352	1.346	0.854	0.850
4	2.260			2.259	2.248	1.279	1.273		
6	3.089			3.061	3.082	1.651	1.677		
8	3.879			3.862	3.875	2.048	2.066		
10	4.641			4.646	4.638	2.446	2.442		
15	6.431			6.431	6.459	3.327	3.344		
20	8.198			8.145	8.197	4.181	4.207		

To further compare the performance of the numerical method and analytical solution, the relative error based on Q_{A4} for the numerical method is calculated by Equation (27), as plotted in Figure 4. In Figure 4a,b, δ_{N1} varies from -0.8% to 2.5% and $\delta_{N2(\beta=0)}$ varies from -0.8% to 0.6% . In Figure 4c,d, $\delta_{N2(\beta=0.5)}$ varies from -1.6% to 0.5% . The comparison results show that Q_{N1} and $Q_{N2(\beta=0)}$ are in very good agreement with $Q_{A4(\beta=0)}$, and $Q_{N2(\beta=0.5)}$ is also consistent with $Q_{A4(\beta=0.5)}$, indicating that both analytical solutions and numerical methods have good performance in estimating the water inflow into a circular underwater tunnel with a lining and an EDZ in a semi-infinite aquifer.

In general, the numerical method has the advantage of dealing with the complicate geological and hydrological models with various boundary conditions, while it is more convenient and efficient to conduct parameter sensitivity analysis and summarize the law by using analytical solutions. Therefore, the effect of EDZ on water inflow into the tunnel is analyzed by the analytical solutions in the next section.

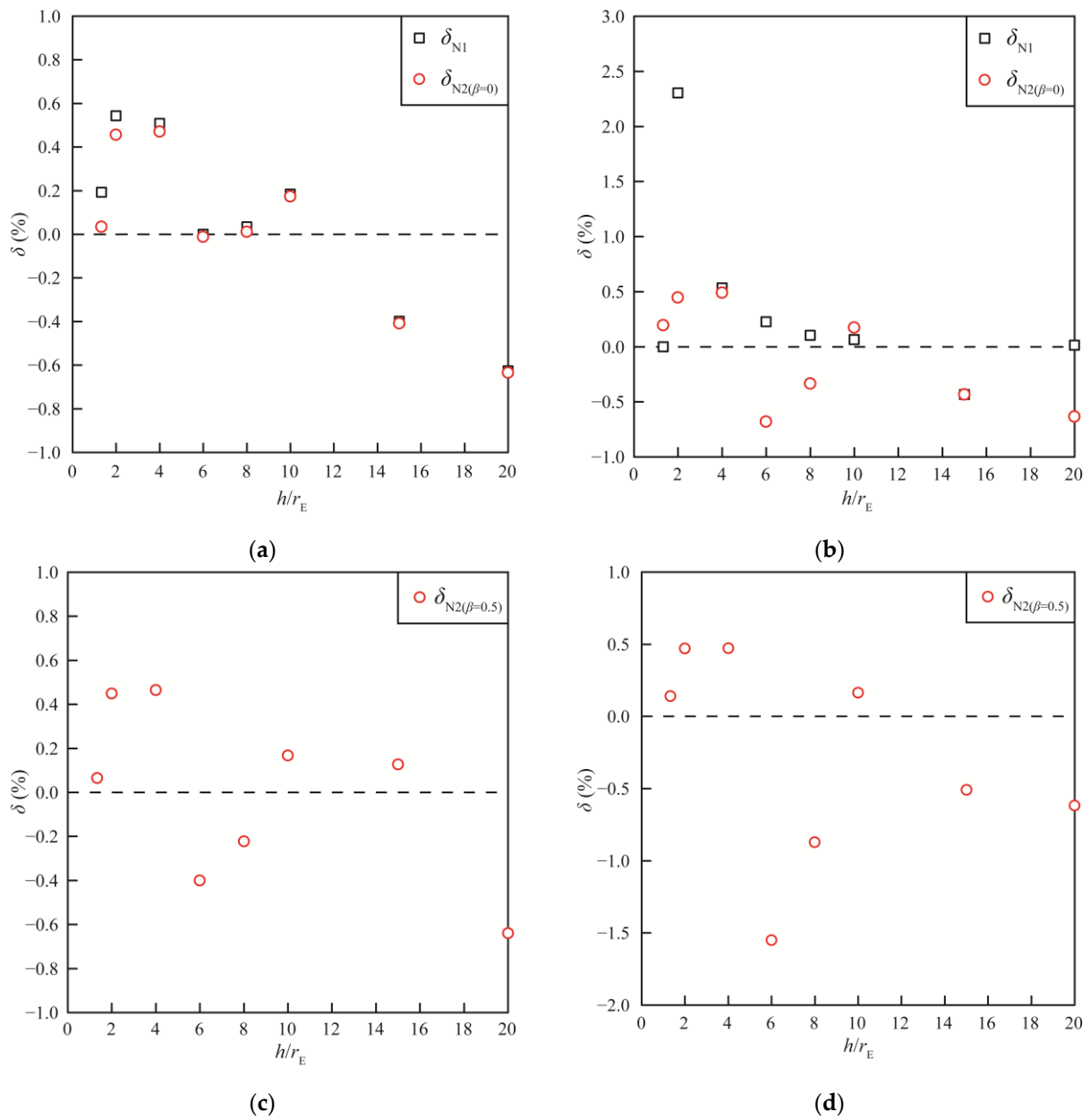


Figure 4. Differences in numerical methods with analytical solutions with various h/r_E values. (a) $H/r_E = 10, k_R/k_L = 10, \beta = 0$; (b) $H/r_E = 0, k_R/k_L = 10, \beta = 0$; (c) $H/r_E = 10, k_R/k_L = 10, \beta = 0.5$; (d) $H/r_E = 0, k_R/k_L = 10, \beta = 0.5$.

4. Discussion

4.1. Effect of EDZ on Water Inflow

As mentioned in the first section, it is very important and useful to determine the effect of the EDZ on water inflow into underwater tunnels for designing a reasonable waterproof and drainage scheme. Hence, an EDZ impact factor is proposed based on Equation (11) in this study, as follows:

$$F_E = \frac{\ln b}{a} + \ln \left[\frac{h}{br_L} + \sqrt{\left(\frac{h}{br_L}\right)^2 - 1} \right] \quad (28)$$

where $a = k_E/k_R$ and $b = r_E/r_L$. a is the ratio of the permeability coefficient of the EDZ to the permeability coefficient of the surrounding rock ($a \geq 1$), and b is the ratio of the radius of the EDZ to the radius of the lining ($b \geq 1$). Then, Equation (11) can be rewritten as

$$Q_{A2} = \frac{2\pi k_R(H + h - h_0)}{F_E + \frac{k_R}{k_L} \ln \frac{r_L}{r_0}} \tag{29}$$

For Equation (29), the ratio of water inflow into the tunnel with EDZ (Q) to the water inflow into the tunnel without EDZ (Q_0) can be estimated as follows:

$$\frac{Q}{Q_0} = \frac{F_{E0} + \frac{k_R}{k_L} \ln \frac{r_L}{r_0}}{F_E + \frac{k_R}{k_L} \ln \frac{r_L}{r_0}} \tag{30}$$

where $F_{E0} = F_{E(b=1)} = \ln \left[h/r_L + \sqrt{(h/r_L)^2 - 1} \right]$.

According to Equation (30), the effect of the EDZ on water inflow into the tunnel can be evaluated based on F_E/F_{E0} values. The variation in F_E/F_{E0} with different parameters a and b is shown in Figure 5. Parameter a represents the ratio of permeability coefficient between the EDZ and the surrounding rock. Parameter b represents the ratio of radius between the EDZ and the lining.

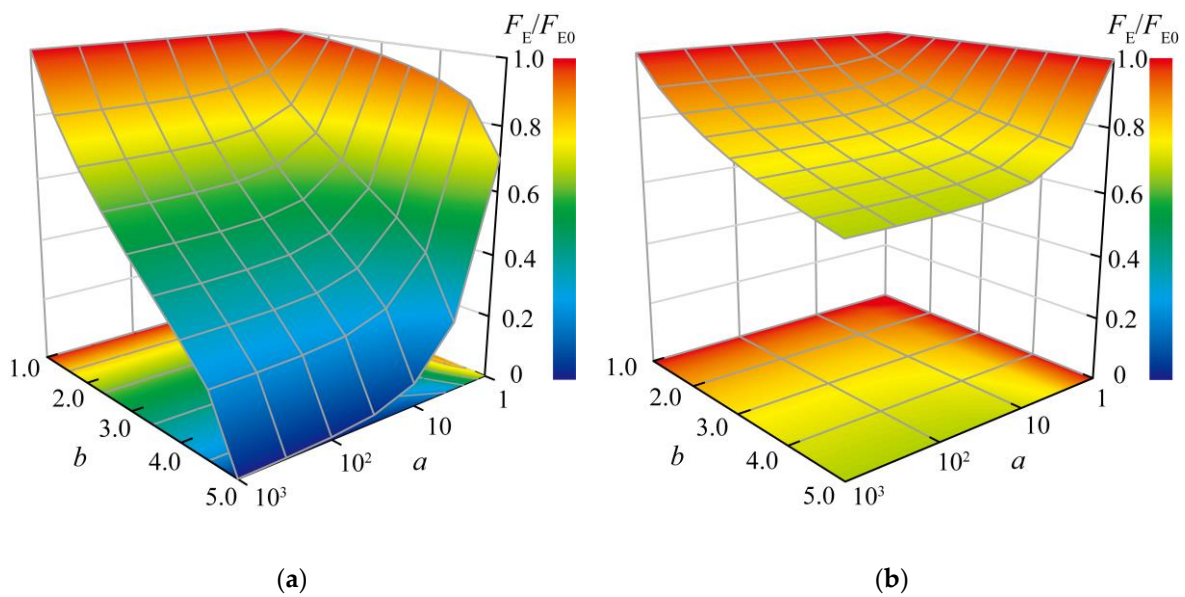


Figure 5. Variation in F_E/F_{E0} with parameters a and b . (a) $h/r_L = 5$; (b) $h/r_L = 50$.

As shown in Figure 5, F_E/F_{E0} decreases with increasing parameters a and b . F_E/F_{E0} is always equal to 1, regardless of the value of a and h/r_L when $b = 1$. When $b = 5$ and $h/r_L = 5$, F_E/F_{E0} decreases from 70.21% to 0.07%, as a increases from 1 to 1000. When $b = 5$ and $h/r_L = 50$, F_E/F_{E0} decreases from 99.95% to 65.03%, as a increases from 1 to 1000. The results above suggest that F_E/F_{E0} decreases with increasing a , and the variation amplitude of F_E/F_{E0} increases as the EDZ becomes thicker and h/r_L decreases.

On the one hand, F_E/F_{E0} decreases from 100% to 70.21% as b increases from 1 to 5, when $a = 1$ and $h/r_L = 5$, and it decreases from 100% to 99.95% as b increases from 1 to 5, when $a = 1$ and $h/r_L = 50$. On the other hand, F_E/F_{E0} decreases from 100% to 0.07% as b increases from 1 to 5, when $a = 1000$ and $h/r_L = 5$, and it decreases from 100% to 65.03% as b increases from 1 to 5, when $a = 1000$ and $h/r_L = 50$. The results above indicate that F_E/F_{E0} decreases as the EDZ becomes thicker, and the variation amplitude increases as the permeability of EDZ increases and the h/r_L decreases. Therefore, the variations in EDZ parameters a and b have a greater impact on F_E/F_{E0} as the tunnel is buried more shallowly.

To determine the relationship between Q/Q_0 and F_E/F_{E0} with different k_R/k_L and r_L/r_0 values, a set of calculations are performed, and the results are shown in Figures 6 and 7, respectively. Figures 6 and 7 show that Q/Q_0 increases as F_E/F_{E0} decreases, namely, as a and b increase. The sensitivity of Q/Q_0 to F_E/F_{E0} decreases with increasing k_R/k_L and r_L/r_0 , which indicates that the increase in the impermeability and thickness of the lining can reduce the influence of EDZ on water inflow into the tunnel. Furthermore, the increase in Q/Q_0 is sharp when F_E/F_{E0} changes from 1 to 0.01, but the curve tends to be gentle with a further reduction in F_E/F_{E0} , which means that there is a limit for the effect of EDZ on water inflow into the tunnel.

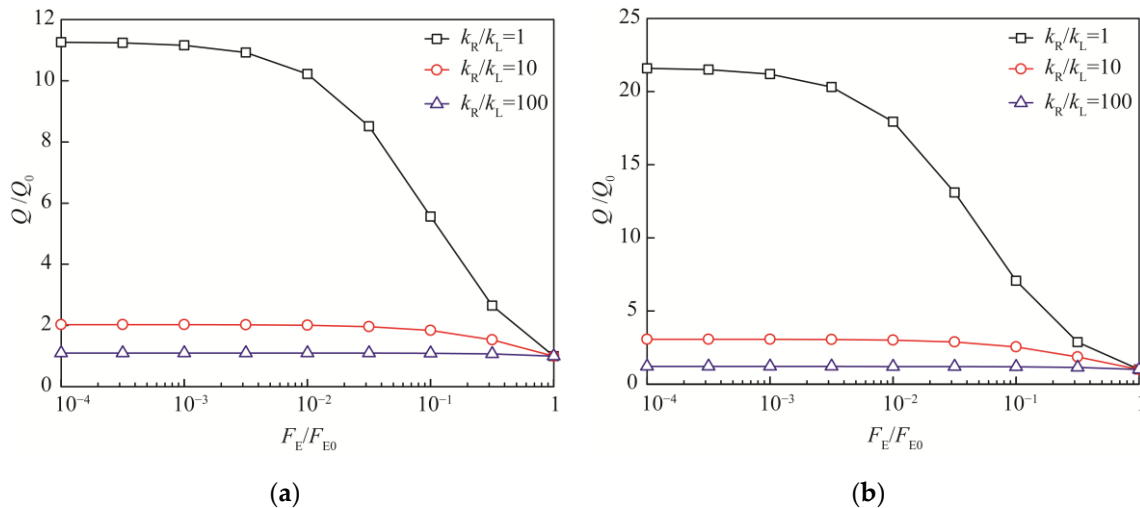


Figure 6. Relationship between Q/Q_0 and F_E/F_{E0} with different k_R/k_L values. (a) $h/r_L = 5$; (b) $h/r_L = 50$.

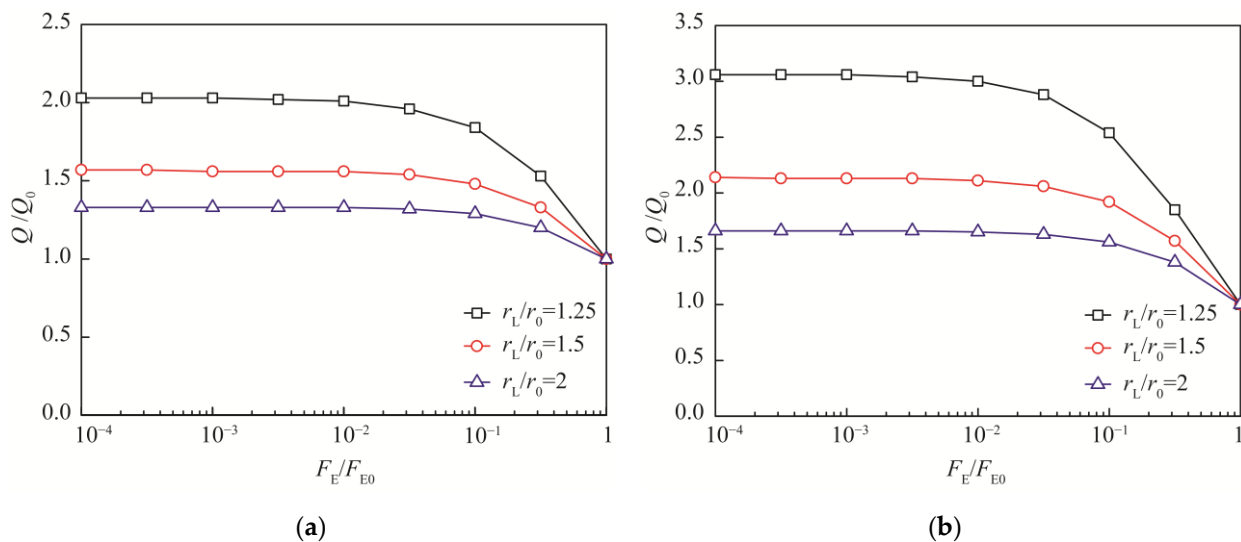


Figure 7. Relationship between Q/Q_0 and F_E/F_{E0} with different r_L/r_0 values. (a) $h/r_L = 5$; (b) $h/r_L = 50$.

According to Figures 6 and 7, the Q/Q_0 of the deep tunnel is greater than that of shallow tunnel when F_E/F_{E0} is the same. However, the opposite phenomenon is observed when the EDZ parameters are the same because F_E/F_{E0} is more sensitive to the variations in EDZ parameters for shallow tunnels, as shown in Table 4. In addition, the difference in Q/Q_0 between tunnels with h/r_L values of 5 and 50 decreases significantly when k_R/k_L increases by 10 times, when comparing the data of the first group and the second group in Table 4. Similarly, the difference in Q/Q_0 between shallow and deep tunnels decreases

with the increasing r_L/r_0 values, when comparing the data of the first group and the third group in Table 4.

Table 4. Computational analyses for Q/Q_0 with different h/r_L , k_R/k_L and r_L/r_0 values.

Scheme No.	h/r_L	a	b	F_E/F_{E0}	k_R/k_L	r_L/r_0	Q/Q_0
1	5	1000	5	0.07%	1	1.25	11.19
	50	1000	5	65.03%	1	1.25	1.50
2	5	1000	5	0.07%	10	1.25	2.03
	50	1000	5	65.03%	10	1.25	1.31
3	5	1000	5	0.07%	1	2	4.30
	50	1000	5	65.03%	1	2	1.44

4.2. Effect Evaluation in Real Engineering Case

According to the above analysis, the effect of EDZ on water inflow into underwater tunnels cannot be ignored. To provide practical insight into the effect of EDZ, the water inflow into the Qingdao Jiaozhou Bay Subsea Tunnel is calculated by Equation (11), and the effect of the EDZ is evaluated by Equation (30), based on the data from the literature [8]. The parameters of the Qingdao Jiaozhou Bay Subsea Tunnel are listed in Table 5, and the parameters of sections and evaluation results are shown in Table 6. In this study, the EDZ parameters a and b are taken as 10 and 1.5, with reference to the numerical simulation in the Section 3 due to the lack of field measurement data of the EDZ.

Table 5. Parameters of Qingdao Jiaozhou Bay Subsea Tunnel.

r_0 (m)	r_L (m)	k_L (m/s)	a	b
8	9	1×10^{-7}	10	1.5

Table 6. Parameters of sections and evaluation results.

No.	Mileage	k_R (m/s)	h (m)	H (m)	Q ($m^3 \cdot d^{-1} \cdot m^{-1}$)	Q/Q_0
1	ZK3 + 125–ZK3 + 325	1.74×10^{-7}	27	0	1.629	1.259
2	ZK3 + 325–ZK3 + 595	8.1×10^{-7}	30.3	5	6.356	1.162
3	ZK3 + 595–ZK3 + 932	4.63×10^{-7}	40.6	5.3	4.906	1.162
4	ZK3 + 932–ZK4 + 102	3.47×10^{-7}	46.4	6.6	4.241	1.160
5	ZK4 + 102–ZK4 + 362	4.63×10^{-7}	44.9	12.4	5.860	1.154
6	ZK4 + 362–ZK4 + 422	1.5×10^{-6}	44.9	16.1	13.520	1.103
7	ZK4 + 422–ZK4 + 562	4.05×10^{-7}	43.7	19.8	5.915	1.161
8	ZK4 + 562–ZK4 + 627	6.94×10^{-7}	43.64	21.86	9.145	1.140
9	ZK4 + 627–ZK4 + 917	3.47×10^{-7}	43.24	26.26	5.742	1.166
10	ZK4 + 917–ZK4 + 977	4.63×10^{-7}	43.5	29.3	7.548	1.156
11	ZK4 + 977–ZK5 + 022	4.63×10^{-7}	43.86	30.64	7.697	1.156
12	ZK5 + 022–ZK5 + 212	9.26×10^{-7}	44.37	33.43	13.08	1.127
13	ZK5 + 212–ZK5 + 372	3.47×10^{-7}	43	37.2	6.643	1.167
14	ZK5 + 372–ZK5 + 482	1.16×10^{-7}	41.7	40.8	2.631	1.193
15	ZK5 + 482–ZK6 + 082	1.16×10^{-7}	40.5	42.4	2.685	1.197

The Q/Q_0 evaluated with the corresponding water inflow is plotted in Figure 8, where Q/Q_0 ranges from 1.103 to 1.259 in these 15 sections of the Qingdao Jiaozhou Bay Subsea Tunnel. The maximum Q/Q_0 occurs in section No.1, with a Q value of $1.629 m^3 \cdot d^{-1} \cdot m^{-1}$, and the minimum Q/Q_0 occurs in section No.6, with a Q value of $13.52 m^3 \cdot d^{-1} \cdot m^{-1}$. To further investigate the relationship, the variation in Q/Q_0 with the magnitude of water inflow into tunnel Q is illustrated in Figure 9, which shows that Q/Q_0 depends on Q via a power function. In Figure 9, the effect of EDZ decreases with the increase in magnitude of water inflow into the tunnel, and the rate of variation decreases gradually, indicating that the effect of EDZ is stronger for underwater tunnels with small water inflow and stabilizes as the magnitude of water inflow increases. In addition, the evaluation results,

based on the Qingdao Jiaozhou Bay Subsea Tunnel, suggest that the EDZ increases the water inflow into a tunnel by at least 10%, even if the lining is applied, and it is necessary to consider the effect of EDZ carefully for estimating the water inflow into an underwater tunnel. It is worth mentioning that there is no relation between Q/Q_0 and the depth of water H according to Equation (30), but the initial water inflow Q_0 increases as H increases, which means that a greater water inflow Q occurs in an underwater tunnel with a greater water depth.

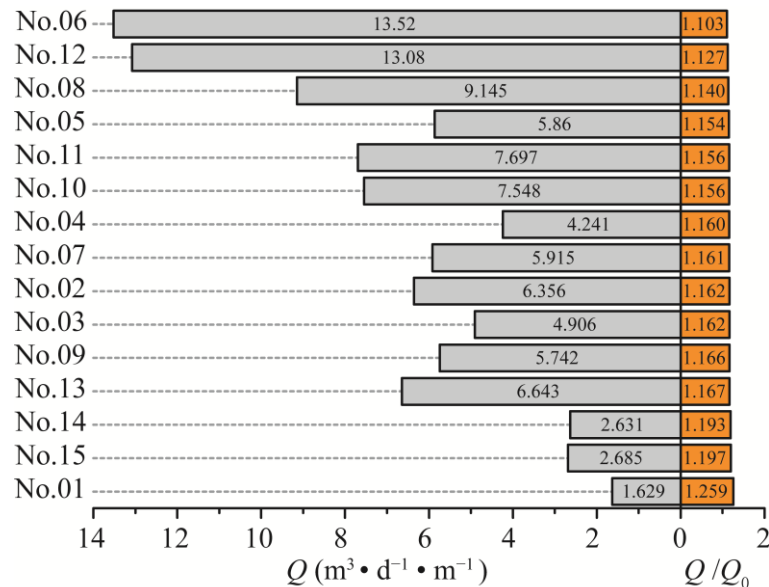


Figure 8. Q/Q_0 values with corresponding water inflow Q values in Qingdao Jiaozhou Bay Sub-sea Tunnel.

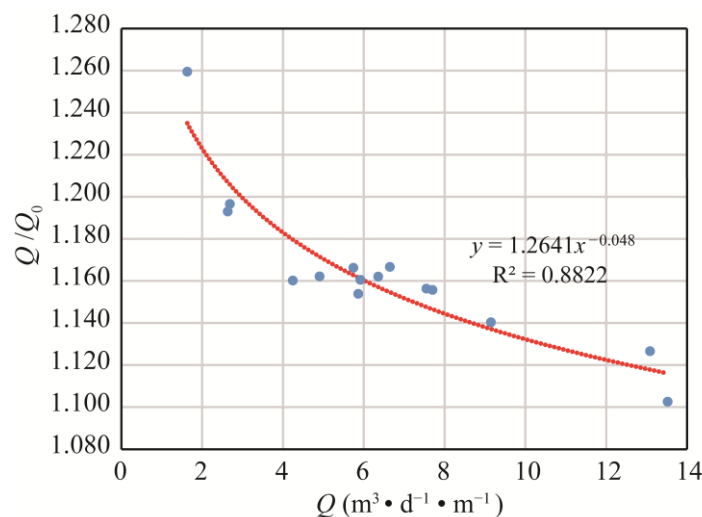


Figure 9. Variation in Q/Q_0 values with the magnitude of water inflow Q .

4.3. Seepage-Preventing Effect of Grouting

Considering that the water inflow into the tunnel and the risk of water intrush increase due to the existence of the EDZ, it is necessary to take seepage-preventing measures to reduce the effect of EDZ. Grouting reinforcement during tunnel excavation can effectively improve the impermeability of the EDZ and reduce the water inflow into the tunnel. Based on the simplified model of water inflow into underwater tunnels with an EDZ (Figure 1), when the radius of the grouting circle is equal to or greater than the radius of EDZ, the analytical solution for water inflow into an underwater tunnel with a grouting circle can be

obtained by replacing k_E and r_E in Equation (11) with k_G and r_G . The seepage-preventing effect of grouting can be estimated by the ratio of water inflow into the tunnel with a grouting circle (Q_G) to water inflow into the tunnel with an EDZ (Q), as follows:

$$\frac{Q_G}{Q} = \frac{\frac{k_R}{k_E} \ln \frac{r_E}{r_L} + \frac{k_R}{k_L} \ln \frac{r_L}{r_0} + \ln \frac{h + \sqrt{h^2 - r_E^2}}{r_E}}{\frac{k_R}{k_G} \ln \frac{r_G}{r_L} + \frac{k_R}{k_L} \ln \frac{r_L}{r_0} + \ln \frac{h + \sqrt{h^2 - r_G^2}}{r_G}} \quad (31)$$

A series of computational analyses for Q_G/Q with different grouting parameters are performed based on Equation (31) and the input data of computational analyses are listed in Table 7. The results of computational analyses are illustrated in Figure 10. According to the results of the first group, when $k_R/k_E = 0.1$, Q_G/Q decreases from 67.32% to 16.95% as k_R/k_G increases from 10 to 100, which suggests that the increase in the impermeability of the grouting circle can reduce the effect of EDZ on water inflow. Similarly, the results of the second group show that Q_G/Q decreases from 67.02% to 50.39% as r_G/r_L increases from 2 to 4, when $k_R/k_E = 0.01$, which means that the water inflow into the tunnel can be reduced by increasing the thickness of the grouting circle. The variation range of the permeability of the grouting circle is much larger than that of its thickness in practical engineering. Hence, reducing the water inflow by improving the impermeability of the grouting circle on the premise of $r_G \geq r_E$ is preferred. Moreover, the results of the third group indicate that the initial values of k_R/k_E and r_E/r_L have little effect on Q_G/Q .

Table 7. Input data of computational analyses for Q_G/Q with different grouting parameters.

Scheme No.	k_R/k_E	r_E/r_L	k_R/k_G	r_G/r_L	k_R/k_L	r_L/r_0	h/r_E	h/r_G
1	0.1	2	10	2	10	1.25	2.5	2.5
	0.1	2	100	2	10	1.25	2.5	2.5
2	0.01	2	10	2	10	1.25	2.5	2.5
	0.01	2	10	4	10	1.25	2.5	2.5
3	0.1	4	10	4	10	1.25	1.25	1.25
	0.1	2	10	4	10	1.25	1.25	1.25
	0.01	2	10	4	10	1.25	1.25	1.25

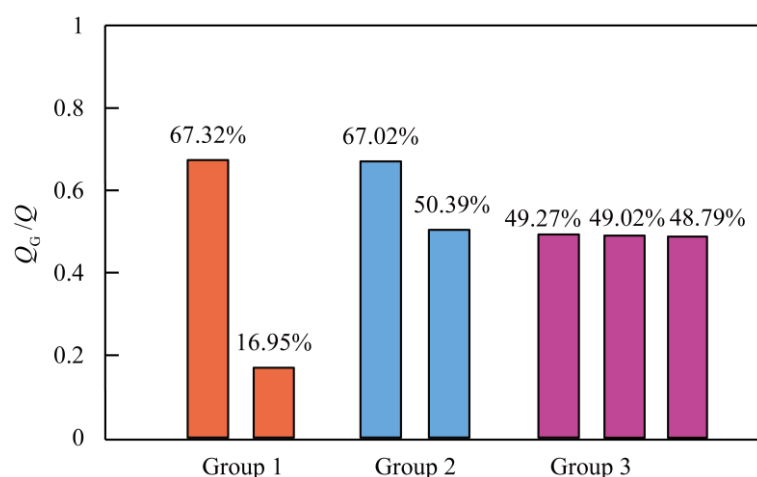


Figure 10. Q_G/Q values with different grouting parameters.

The above discussion on reducing the effect of the EDZ with grouting reinforcement is for a general model with simplified conditions. According to the previous studies [37–42], the changes in rock permeability caused by excavation damage depend on a variety of conditions, including the initial stress field, the properties of rock, the natural fracture zones and the excavation methods. Therefore, in order to put forward the specific anti-seepage

measures for a real engineering case, a detailed study on how excavation damage causes the changes in rock permeability should be conducted based on field and indoor tests in the future.

5. Conclusions

In this study, both analytical solutions and numerical methods are applied to estimate the steady-state water inflow into a circular underwater tunnel with an EDZ. The comparison results show that both analytical solutions and numerical methods have good performance. An impact factor of the EDZ is proposed, and the effect of EDZ on water inflow into the tunnel is analyzed by using the analytical solution due to its convenience. Finally, a series of parameter analyses is performed, and some main conclusions are summarized as follows:

1. The F_E/F_{E0} ratio decreases as the permeability and thickness of the EDZ increase, and the variation amplitude increases with the decrease in h/r_L . Hence, the variations in EDZ parameters a and b have a greater impact on F_E/F_{E0} , as the tunnel is buried more shallowly.
2. The Q/Q_0 ratio increases as F_E/F_{E0} decreases, namely, as a and b increase. However, there is a limit for the influence of the EDZ on water inflow into the tunnel, and the increase in the impermeability and thickness of the lining can reduce the effect of the EDZ on water inflow.
3. The difference in Q/Q_0 values between deep and shallow tunnels decreases with increasing impermeability and lining thickness. Furthermore, the effect of the EDZ is stronger for underwater tunnels with small water inflows and stabilizes as the magnitude of the water inflow increases.
4. Grouting is an effective measure to eliminate the effect of the EDZ on water inflow into tunnels. The increase in the impermeability and thickness of the grouting circle can reduce water inflow into the tunnel, and the initial values of k_R/k_E and r_E/r_L have little effect on Q_G/Q . In addition, reducing the water inflow by improving the impermeability of the grouting circle on the premise of $r_G \geq r_E$ in practical engineering is preferred.

Author Contributions: Conceptualization, Y.-H.P. and J.-R.Q.; Methodology, Y.-H.P. and J.-F.Z.; Validation, Y.-X.P. and C.C.; Writing—original draft preparation, Y.-H.P. and J.-R.Q.; Writing—review and editing, H.-N.M. and C.Y.; Funding acquisition, Y.-H.P. and J.-R.Q. All authors have read and agreed to the published version of the manuscript.

Funding: This study was funded by the National Key Research and Development Program of China (Grant No. 2021YFB2601100), the National Natural Science Foundation of China (Grant No. 52109087), the Natural Science Foundation of Fujian (Grant No. 2020J05145), the Education Department of Fujian (Grant No. JAT190305, JAT190306 & KL41806), the Science Foundation of Jimei University (Grant No. ZQ2019009), and the Science and Technology R&D Program of China Construction Infrastructure Co., Ltd. (Grant No. CSCIC-2021-KT-02). The authors gratefully appreciate the support provided.

Data Availability Statement: The data presented in this study are available upon request from the corresponding author.

Conflicts of Interest: The authors declare no conflict of interest.

References

1. Coli, M.; Pinzani, A. Tunnelling and hydrogeological issues: A short review of the current state of the art. *Rock Mech. Rock Eng.* **2014**, *47*, 839–851. [[CrossRef](#)]
2. Nilsen, B. Characteristics of water ingress in Norwegian subsea tunnels. *Rock Mech. Rock Eng.* **2014**, *47*, 933–945. [[CrossRef](#)]
3. Zhao, J.; Tan, Z.; Ma, N. Development and application of a new reduction coefficient of water pressure on sub-sea tunnel lining. *Appl. Sci.* **2022**, *12*, 2496. [[CrossRef](#)]
4. Peng, Y.; Wu, L.; Zuo, Q.; Chen, C.; Hao, Y. Risk assessment of water inrush in tunnel through water-rich fault based on AHP-Cloud model. *Geomat. Nat. Hazards Risk* **2020**, *11*, 301–317. [[CrossRef](#)]

5. Liu, R.; Liu, Y.; Xin, D.; Li, S.; Zheng, Z.; Ma, C.; Zhang, C. Prediction of water inflow in subsea tunnels under blasting vibration. *Water* **2018**, *10*, 1336. [[CrossRef](#)]
6. Cao, Y.; Jiang, J.; Xie, K.; Huang, W. Analytical solutions for nonlinear consolidation of soft soil around a shield tunnel with idealized sealing linings. *Comput. Geotech.* **2014**, *61*, 144–152. [[CrossRef](#)]
7. Shin, Y.; Song, K.; Lee, I.; Cho, G. Interaction between tunnel supports and ground convergence—Consideration of seepage forces. *Int. J. Rock Mech. Min.* **2011**, *48*, 394–405. [[CrossRef](#)]
8. Yang, G.; Wang, X.; Wang, X.; Cao, Y. Analyses of seepage problems in a subsea tunnel considering effects of grouting and lining structure. *Mar. Georesour. Geotec.* **2016**, *34*, 65–70. [[CrossRef](#)]
9. Zhang, D.M.; Huang, Z.K.; Yin, Z.Y.; Ran, L.Z.; Huang, H.W. Predicting the grouting effect on leakage-induced tunnels and ground response in saturated soils. *Tunn. Undergr. Space Technol.* **2017**, *65*, 76–90. [[CrossRef](#)]
10. Farhadian, H.; Nikvar-Hassani, A. Water flow into tunnels in discontinuous rock: A short critical review of the analytical solution of the art. *Bull. Eng. Geol. Environ.* **2019**, *78*, 3833–3849. [[CrossRef](#)]
11. Fernandez, G.; Moon, J. Excavation-induced hydraulic conductivity reduction around a tunnel—Part 1: Guideline for estimate of ground water inflow rate. *Tunn. Undergr. Space Technol.* **2010**, *25*, 560–566. [[CrossRef](#)]
12. Bai, Y.; Wu, Z.; Huang, T.; Peng, D. A Dynamic modeling approach to predict water inflow during karst tunnel excavation. *Water* **2022**, *14*, 2380. [[CrossRef](#)]
13. Li, P.; Wang, F.; Long, Y.; Zhao, X. Investigation of steady water inflow into a subsea grouted tunnel. *Tunn. Undergr. Space Technol.* **2018**, *80*, 92–102. [[CrossRef](#)]
14. Moon, J.; Fernandez, G. Effect of excavation-induced groundwater level drawdown on tunnel inflow in a jointed rock mass. *Eng. Geol.* **2010**, *110*, 33–42. [[CrossRef](#)]
15. Butscher, C. Steady-state groundwater inflow into a circular tunnel. *Tunn. Undergr. Space Technol.* **2012**, *32*, 158–167. [[CrossRef](#)]
16. Farhadian, H.; Nikvar Hassani, A.; Katibeh, H. Groundwater inflow assessment to Karaj Water Conveyance tunnel, northern Iran. *KSCE J. Civ. Eng.* **2017**, *21*, 2429–2438. [[CrossRef](#)]
17. Fernandez, G.; Moon, J. Excavation-induced hydraulic conductivity reduction around a tunnel—Part 2: Verification of proposed method using numerical modeling. *Tunn. Undergr. Space Technol.* **2010**, *25*, 567–574. [[CrossRef](#)]
18. Nikvar Hassani, A.; Farhadian, H.; Katibeh, H. A comparative study on evaluation of steady-state groundwater inflow into a circular shallow tunnel. *Tunn. Undergr. Space Technol.* **2018**, *73*, 15–25. [[CrossRef](#)]
19. Nikvar Hassani, A.; Katibeh, H.; Farhadian, H. Numerical analysis of steady-state groundwater inflow into Tabriz line 2 metro tunnel, northwestern Iran, with special consideration of model dimensions. *Bull. Eng. Geol. Environ.* **2016**, *75*, 1617–1627. [[CrossRef](#)]
20. Farhadian, H.; Katibeh, H.; Huggenberger, P. Empirical model for estimating groundwater flow into tunnel in discontinuous rock masses. *Environ. Earth Sci.* **2016**, *75*, 417. [[CrossRef](#)]
21. Gattinoni, P.; Scesi, L. An empirical equation for tunnel inflow assessment: Application to sedimentary rock masses. *Hydrogeol. J.* **2010**, *18*, 1797–1810. [[CrossRef](#)]
22. Wang, X.; Tan, Z.; Wang, M.; Zhang, M.; Ming, H. Theoretical and experimental study of external water pressure on tunnel lining in controlled drainage under high water level. *Tunn. Undergr. Space Technol.* **2008**, *23*, 552–560. [[CrossRef](#)]
23. Huangfu, M.; Wang, M.; Tan, Z.; Wang, X. Analytical solutions for steady seepage into an underwater circular tunnel. *Tunn. Undergr. Space Technol.* **2010**, *25*, 391–396. [[CrossRef](#)]
24. Harr, M.E. *Groundwater and Seepage*; McGraw-Hill: New York, NY, USA, 1962.
25. Goodman, R.E.; Moye, D.G.; Schalkwyk, A.; Javandel, I. Ground water inflow during tunnel driving. *Eng. Geol.* **1965**, *2*, 39–56.
26. Lei, S. An analytical solution for steady flow into a tunnel. *Ground Water* **1999**, *37*, 23–26. [[CrossRef](#)]
27. Ying, H.; Zhu, C.; Gong, X. Analytic solution on seepage field of underwater tunnel considering grouting circle. *J. Zhejiang Univ. Eng. Sci.* **2016**, *50*, 1018–1023.
28. Su, K.; Zhou, Y.; Wu, H.; Shi, C.; Zhou, L. An analytical method for groundwater inflow into a drained circular tunnel. *Ground Water* **2017**, *55*, 712–721. [[CrossRef](#)]
29. El Tani, M. Circular tunnel in a semi-infinite aquifer. *Tunn. Undergr. Space Technol.* **2003**, *18*, 49–55. [[CrossRef](#)]
30. Kolymbas, D.; Wagner, P. Groundwater ingress to tunnels—The exact analytical solution. *Tunn. Undergr. Space Technol.* **2007**, *22*, 23–27. [[CrossRef](#)]
31. Park, K.; Owatsiriwong, A.; Lee, J. Analytical solution for steady-state groundwater inflow into a drained circular tunnel in a semi-infinite aquifer: A revisit. *Tunn. Undergr. Space Technol.* **2008**, *23*, 206–209. [[CrossRef](#)]
32. Ying, H.; Zhu, C.; Shen, H.; Gong, X. Semi-analytical solution for groundwater ingress into lined tunnel. *Tunn. Undergr. Space Technol.* **2018**, *76*, 43–47. [[CrossRef](#)]
33. Du, C.; Wang, M.; Tan, Z. Analytical solution for seepage field of subsea tunnel and its application. *Chin. J. Rock Mech. Eng.* **2011**, *30*, 3567–3573.
34. Li, P.; Zhang, D.; Zhao, Y.; Zhang, C. Study of distribution law of water pressure acting on composite lining and reasonable parameters of grouting circle for subsea tunnel. *Chin. J. Rock Mech. Eng.* **2012**, *31*, 280–288.
35. Pan, Y.; Luo, Q.; Zhou, B.; Chen, J. Analytical study on seepage field of deep tunnel with grouting circle in half plane. *J. Zhejiang Univ. Eng. Sci.* **2018**, *52*, 1114–1122.

36. Zhu, C.; Ying, H.; Gong, X. Analytical solutions for seepage fields of underwater tunnels with arbitrary burial depth. *Chin. J. Geotech. Eng.* **2017**, *39*, 1984–1991.
37. Butscher, C.; Einstein, H.H.; Huggenberger, P. Effects of tunneling on groundwater flow and swelling of clay-sulfate rocks. *Water Resour. Res.* **2011**, *47*, 1–17. [[CrossRef](#)]
38. Peng, Y.; Liu, G.; Wu, L.; Zuo, Q.; Liu, Y.; Zhang, C. Comparative study on tunnel blast-induced vibration for the underground cavern group. *Environ. Earth Sci.* **2021**, *80*, 68. [[CrossRef](#)]
39. Martino, J.B.; Chandler, N.A. Excavation-induced damage studies at the Underground Research Laboratory. *Int. J. Rock Mech. Min.* **2004**, *41*, 1413–1426. [[CrossRef](#)]
40. Tsang, C.; Bernier, F.; Davies, C. Geohydromechanical processes in the Excavation Damaged Zone in crystalline rock, rock salt, and indurated and plastic clays—In the context of radioactive waste disposal. *Int. J. Rock Mech. Min.* **2005**, *42*, 109–125. [[CrossRef](#)]
41. Souley, M.; Homand, F.; Pepa, S.; Hoxha, D. Damage-induced permeability changes in granite: A case example at the URL in Canada. *Int. J. Rock Mech. Min.* **2001**, *38*, 297–310. [[CrossRef](#)]
42. Bossart, P.; Meier, P.M.; Moeri, A.; Trick, T.; Mayor, J. Geological and hydraulic characterisation of the excavation disturbed zone in the Opalinus Clay of the Mont Terri Rock Laboratory. *Eng. Geol.* **2002**, *66*, 19–38. [[CrossRef](#)]
43. Schleiss, A. Design of reinforced concrete linings of pressure tunnels and shafts. *Int. J. Hydropower Dams* **1997**, *4*, 88–94.